Spin polarization on Fermi surfaces of metals by the KKR method

Martin Gradhand,[1,2,*] Michael Czerner,[2] Dmitry V. Fedorov,[2] Peter Zahn,[2] Bogdan Yu. Yavorsky,[2] László Szunyogh,[3] and Ingrid Mertig[2,1]

[1]*Max-Planck-Institut für Mikrostrukturphysik, Weinberg 2, D-06120 Halle, Germany*

[2]*Institut für Physik, Martin-Luther-Universität Halle–Wittenberg, D-06099 Halle, Germany*

[3]*Department of Theoretical Physics, Budapest University of Technology and Economics, H-1521 Budapest, Hungary*

(Received 21 September 2009; revised manuscript received 29 October 2009; published 11 December 2009)

With the implementation of a relativistic Korringa-Kohn-Rostoker Green's function and band-structure method, we analyze the spin-expectation value of the electron states on the Fermi surface of nonmagnetic as well as magnetic metals. It is shown that for relatively light elements such as Cu the spin states are well defined. A separation of all electron states to "up" and "down" spin-polarized states can be done even in the case of quite heavy but monovalent elements such as Au. In contrast, for heavy polyvalent metals such as Pt, the expectation value of the spin operator can be close to zero in large regions of the Fermi surface. In this case the nonrelativistic language of well-defined "spin-up" and "spin-down" states is not valid anymore. For magnetic materials, the relativistic Fermi surfaces change their topology with respect to the nonrelativistic majority and minority sheets because of spin-orbit driven avoided crossings of the bands. As a result, regions with vanishing spin polarization appear.

DOI: 10.1103/PhysRevB.80.224413 PACS number(s): 71.15.−m, 71.18.+y, 71.20.−b

I. INTRODUCTION

The spin degree of freedom of an electron has attracted a lot of attention over the last years.[1–6] Since the field of spintronics opened new perspectives in data storage and information technology. After the discovery of giant magnetoresistance,[7,8] tunneling magnetoresistance,[9–12] and current-induced switching,[13–16] phenomena such as spin Hall effect[1,4,17,18] and anomalous Hall effect[19–22] attracted attention. The latter effects are caused by spin-orbit interaction. Thus, a detailed insight into the microscopic origin requires a relativistic description of the electron system.

While the intrinsic contribution to the anomalous Hall conductivity was discussed originally in terms of an integral of the Berry curvature over all occupied states, it was later shown that for low temperatures this quantity can be expressed as a Fermi-surface property.[23,24] The same holds for the spin Hall effect in nonmagnetic materials. For an understanding of these effects the spin degree of freedom of an electron state is an important quantity. Experimentally, the spin orientation can be changed with respect to the lattice structure either by spin injection from a ferromagnet into a nonmagnetic material or by an external magnetic field. As a consequence spin-flip scattering is observed to be anisotropic.[25] To account for related effects, we present a method to analyze the spin-expectation value of the electronic states at the Fermi surface within a fully relativistic (FR) treatment.

A further motivation for our work is the existence of so-called spin hot spots. They are characterized by zero spin polarization and occur at the Fermi surface.[26] Level crossings at the zone boundary or at high-symmetry points, or lines of accidental degeneracy are typical locations on the Fermi surface. Spin hot spots exist usually for polyvalent metals such as Al, Pd, Mg, and Be and cause an unexpected fast spin relaxation.[26]

For magnetic materials the spin hot spots are caused by spin-orbit driven hybridization points, i.e., **k** points with avoided crossing. That is, the considered states would be degenerate in a nonrelativistic (NR) treatment, "spin-up" and "spin-down" bands cross each other. Spin-orbit interaction forces a splitting of the two states and the spin polarization vanishes at the splitting points. If such points occur close to the Fermi level, they can enhance spin-flip scattering by several orders of magnitude and cause ultrafast demagnetization.[27] For a theoretical study of this problem, it is very desirable to know the spin-mixing parameter of the electron states in the vicinity of the Fermi level.[28]

The aim of this paper is to introduce our *ab initio* method that provides a scheme for the calculation of the relativistic band structure and wave functions. In the application of this method, we present relativistic Fermi surfaces and consider the spin polarization of the corresponding electronic states.

We start with a short introduction of the relativistic Korringa-Kohn-Rostoker (KKR) band-structure theory[29–38] and discuss the treatment of degenerate bands in a nonmagnetic system with space inversion symmetry. For the Fermi-surface calculation, we present Cu, Au, and Pt as nonmagnetic and Fe as magnetic examples. Different spin-mixing parameters obtained for several materials will be discussed in detail.

II. METHOD

For the self-consistent procedure, we use a screened KKR-Green's function method,[39,40] generalized relativistically.[35,38] It is based on the density-functional theory in the local spin-density approximation with the parametrization of Vosko *et al.*[41] The magnetic moments are forced to be collinear. An angular momentum cutoff $l_{max}=3$ is used for the Green's function expansion. The relativistic Kohn-Sham-Dirac equation

$$\hat{H}(\mathbf{r})\Psi_{n\mathbf{k}}(\mathbf{r}) = W_n(\mathbf{k})\Psi_{n\mathbf{k}}(\mathbf{r}) \tag{1}$$

with the Hamiltonian

$$\hat{H}(\mathbf{r}) = \frac{\hbar}{i} c\hat{\alpha}\nabla_{\mathbf{r}} + \hat{I}_4 V_{eff}(\mathbf{r}) + \hat{\beta}\boldsymbol{\sigma}\cdot\mathbf{B}_{eff}(\mathbf{r}) + mc^2\hat{\beta} \quad (2)$$

and the 4×4 matrices

$$\hat{\alpha} = \begin{pmatrix} 0 & \boldsymbol{\sigma} \\ \boldsymbol{\sigma} & 0 \end{pmatrix}, \quad \hat{\beta} = \begin{pmatrix} \hat{I}_2 & 0 \\ 0 & -\hat{I}_2 \end{pmatrix}, \quad \hat{I}_4 = \begin{pmatrix} \hat{I}_2 & 0 \\ 0 & \hat{I}_2 \end{pmatrix} \quad (3)$$

is solved. Here $\hat{I}_2$ is the 2×2 unit matrix, n is the band index, and $\mathbf{k}$ is the Bloch vector. First we use the KKR-Green's function method to obtain the scalar potential $V_{eff}(\mathbf{r})$ and the vector of the effective magnetic field $\mathbf{B}_{eff}(\mathbf{r})$ self-consistently. Then, the KKR band-structure method is applied to compute the electron energy spectrum

$$W_n(\mathbf{k}) = E_n(\mathbf{k}) + mc^2. \quad (4)$$

The band structure $E_n(\mathbf{k})$ is calculated on the real energy axis with an angular momentum cutoff $l_{max}=3$. The cluster used to calculate the screened structure constants contained at least 225 atoms depending on the crystal structure.

We have different options to analyze the influence of relativistic effects. First of all, the results of the FR calculation can be compared with the ones obtained from the NR equation. In addition, in the fully relativistic calculation, the spin-orbit interaction can be scaled to zero.[42] This corresponds to the so-called scalar-relativistic approximation (SRA). The scaling of spin-orbit coupling can be performed by a continuous variable x. Calculations without scaling (FR[$x=1$]) and with scaling to zero (FR[$x=0$]) are discussed, respectively.

The relativistic band-structure calculations are performed analogously to the NR case.[43] However, the wave functions are expanded now into spin-angular functions χ_Q as[38]

$$\Psi_{n\mathbf{k}}(\mathbf{r}) = \sum_Q \sum_{Q'} a^n_{Q'}(\mathbf{k}) \begin{pmatrix} g_{QQ'}(r)\chi_Q(\hat{\mathbf{r}}) \\ if_{QQ'}(r)\chi_{\bar{Q}}(\hat{\mathbf{r}}) \end{pmatrix}, \quad (5)$$

where $Q=\{\kappa\mu\}$ and $\bar{Q}=\{-\kappa\mu\}$. The solutions of the radial differential equation in the atomic sphere approximation for the effective potential are $g_{QQ'}(r)$ for the large and $f_{QQ'}(r)$ for the small component, respectively. The band structure $E_n(\mathbf{k})$ is evaluated from the secular KKR equation

$$\det\left|\hat{G}(\mathbf{k},E) - [\Delta\hat{t}(E)]^{-1}\right| = 0 \quad (6)$$

with the screened structural Green's function $\hat{G}(\mathbf{k},E)$ and the difference of the single-site t matrices $\Delta\hat{t}(E)=\hat{t}-\hat{t}_r$ with $\hat{t}_r$ being the t matrix of the reference system formed by repulsive potential wells. The expansion coefficients $a^n_{Q'}(\mathbf{k})$ are calculated from the KKR eigenvalue problem

$$\sum_{Q'} [G_{QQ'}(\mathbf{k},E_n) - [\Delta t^{-1}(E_n)]_{QQ'}]c^n_{Q'}(\mathbf{k}) = 0 \quad (7)$$

via

$$a^n_Q(\mathbf{k}) = \sum_{Q'} [\Delta t^{-1}(E_n)]_{QQ'} c^n_{Q'}(\mathbf{k}). \quad (8)$$

In the case of a nonmagnetic crystal with inversion symmetry every $\mathbf{k}$ state is twofold degenerate.[44,45] Let us label the two orthonormal wave functions corresponding to that degeneracy as $|\Psi^1_{\mathbf{k}}\rangle$ and $|\Psi^2_{\mathbf{k}}\rangle$. All linear combinations of these functions are also solutions at the same energy $E_n(\mathbf{k})$. In the nonrelativistic case one would associate them with spin-up and spin-down states relative to an arbitrary quantization axis. For the relativistic treatment we have to define a quantization axis. In an experimental situation, this axis can be given by a ferromagnet used for injection of spin-polarized electrons. For a theoretical consideration, we can choose, for instance, the z direction as the quantization axis. Then, we apply the following unitary transformation:

$$|\Psi^3_{\mathbf{k}}\rangle = c_1|\Psi^1_{\mathbf{k}}\rangle + c_2|\Psi^2_{\mathbf{k}}\rangle,$$

$$|\Psi^4_{\mathbf{k}}\rangle = -c^*_2|\Psi^1_{\mathbf{k}}\rangle + c^*_1|\Psi^2_{\mathbf{k}}\rangle \quad (9)$$

with $|c_1|^2+|c_2|^2=1$. Here the coefficients c_1 and c_2 should fulfill the conditions of spin alignment along z direction for the two new states

$$\langle\Psi^3_{\mathbf{k}}|\hat{\beta}\sigma_x|\Psi^3_{\mathbf{k}}\rangle = \langle\Psi^3_{\mathbf{k}}|\hat{\beta}\sigma_y|\Psi^3_{\mathbf{k}}\rangle = 0,$$

$$\langle\Psi^4_{\mathbf{k}}|\hat{\beta}\sigma_x|\Psi^4_{\mathbf{k}}\rangle = \langle\Psi^4_{\mathbf{k}}|\hat{\beta}\sigma_y|\Psi^4_{\mathbf{k}}\rangle = 0. \quad (10)$$

In fact, the upper conditions automatically provide the lower one in Eq. (10). Explicit expressions for the coefficients c_1 and c_2 are given in the Appendix. The normalization

$$\langle\Psi^3_{\mathbf{k}}|\Psi^3_{\mathbf{k}}\rangle = \langle\Psi^4_{\mathbf{k}}|\Psi^4_{\mathbf{k}}\rangle = 1 \quad (11)$$

and the orthogonality

$$\langle\Psi^3_{\mathbf{k}}|\Psi^4_{\mathbf{k}}\rangle = 0 \quad (12)$$

are conserved under the unitary transformation in Eq. (9). The choice of the quantization axis in z direction is not unique and any arbitrary direction can be chosen. For the further discussion of the results the expectation value of the z component of the spin with the transformed wave functions

$$P_{\mathbf{k}} = \langle\Psi^3_{\mathbf{k}}|\hat{\beta}\sigma_z|\Psi^3_{\mathbf{k}}\rangle = -\langle\Psi^4_{\mathbf{k}}|\hat{\beta}\sigma_z|\Psi^4_{\mathbf{k}}\rangle \quad (13)$$

will be referred to as spin polarization. For a clear interpretation, as what follows, we shall label the states constructed from the degenerate band with $P_{\mathbf{k}}>0$ by $|\Psi^+_{\mathbf{k}}\rangle$ and those with $P_{\mathbf{k}}<0$ by $|\Psi^-_{\mathbf{k}}\rangle$. In the nonrelativistic case (without spin-orbit coupling) the two states simplify to the degenerate spin-up $|\Psi^+_{\mathbf{k}}\rangle=|\Phi_{\mathbf{k}},\uparrow\rangle$ and spin-down states $|\Psi^-_{\mathbf{k}}\rangle=|\Phi_{\mathbf{k}},\downarrow\rangle$.

III. RESULTS

A. Band structure

First, we present the band-structure calculations to show that our relativistic code works properly. Pt is chosen as a nonmagnetic example since the large atomic number leads to significant relativistic effects in the electronic structure. Figure 1 shows the relativistic band structure of Pt, in comparison to a nonrelativistic approximation which fails for such a heavy element. The electronic structures obtained with the two approaches differ strongly over the whole Brillouin zone. Our relativistic results are in very good agreement to earlier calculations.[46]

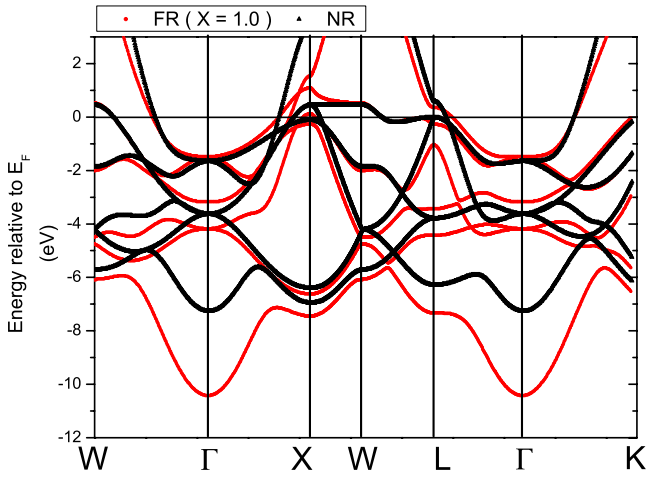

FIG. 1. (Color online) Band structure of Pt from the fully relativistic (gray, red) and the nonrelativistic (black) calculation.

To illuminate the origin of changes in the band structure going from NR to the FR calculation, we perform the FR $[x=0]$ calculation. The results are presented in Fig. 2. Especially, the flat bands are affected and the degeneracy at symmetry points is lifted by the spin-orbit coupling, whereas the band bottom at the Γ point is correctly reproduced within SRA (FR$[x=0]$).

In contrast, the band structure of Fe shown in Fig. 3 is only slightly affected by relativistic effects since Fe is a light element in comparison to Pt. However, the changes are important because some degeneracies are lifted leading to avoided crossings of former majority and minority bands.[46–48] It causes a mixing of bands which were well separated with respect to the spin in the nonrelativistic calculation. This result is especially important for the topology of the Fermi surface and the spin-polarization analysis in the following section.

B. Fermi surface

Here we present the relativistic Fermi surfaces of Cu, Au, Pt, and Fe with the spin polarization of the electronic states.

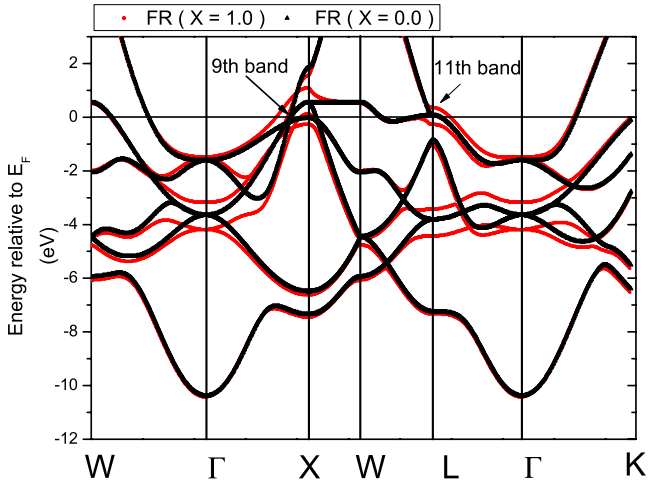

FIG. 2. (Color online) Band structure of Pt from the fully relativistic (gray, red) and the relativistic with the spin-orbit coupling scaled to zero (black) calculation.

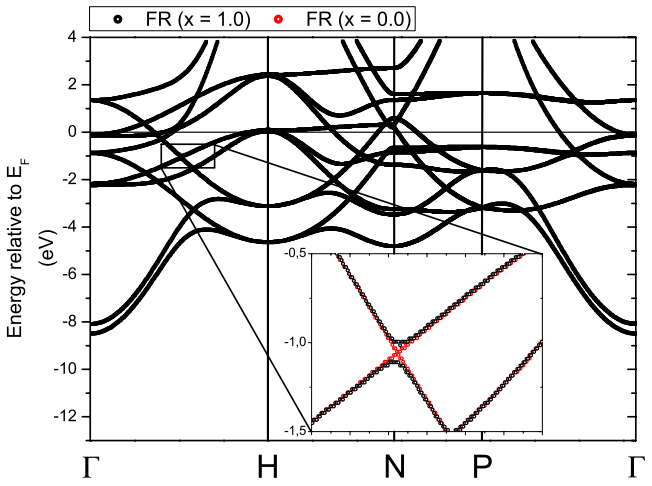

FIG. 3. (Color online) Calculated fully relativistic band structure of bcc Fe. The small inset shows a comparison to the calculation with the spin-orbit coupling scaled to zero ($x=0$). The spin-orbit interaction leads to avoided crossings.

Let us first analyze the polarization of the nonmagnetic Fermi surfaces. The quantization axis is defined by the transformation in Eqs. (9) and (10) explained in Sec. II. The polarization of $|\Psi_{\mathbf{k}}^{+}\rangle$ states only is shown in Fig. 4. A figure for $|\Psi_{\mathbf{k}}^{-}\rangle$ states would look the same but with opposite sign. For the monovalent metals Au and Cu the band at the Fermi level

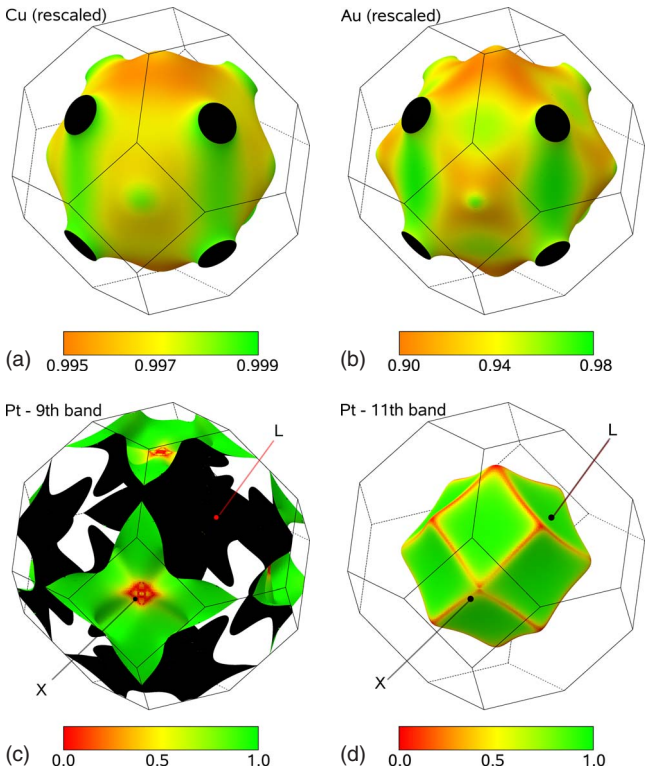

FIG. 4. (Color online) Calculated relativistic Fermi surface of Cu (upper left), Au (upper right), and Pt (lower left: nineth band and lower right: 11th band), and the expectation values of $\hat{\beta}\sigma_z$ for the $|\Psi_k^{+}\rangle$ states are indicated as color code. Note the different scale for Cu and Au in comparison to Pt.

is shown. Pt, which is a polyvalent metal, exhibits a very strong influence of the spin-orbit coupling that can be seen from the shown bands with small spin polarization in large regions of **k** space. All polarization values between 0 and +1 for the $|\Psi_{\mathbf{k}}^{+}\rangle$ states are obtained for Pt. The effect is much weaker for Cu and even for Au. Notice the different scales in Fig. 4. It is important to mention that the symmetry of the spin polarization P is lower than the symmetry of the Fermi surface. The spin degree of freedom is coupled to the lattice because of spin-orbit interaction. The operator $\hat{\beta}\boldsymbol{\sigma}$ does not commute with the relativistic Hamiltonian of Eq. (2) and the chosen quantization axis is reflected in the symmetry. If the transformation is applied using the quantization axis along x, the pictures in Fig. 4 would be rotated by 90° around y axis.

There are two reasons why the influence of the spin-orbit coupling is increased. First, Au and Pt are heavier than Cu with atomic numbers of $Z=79$ and $Z=78$ in comparison to $Z=29$. Since the spin-orbit coupling strength is proportional to Z, the effect in Pt and Au is stronger. Second, the band structure affects directly the strength of the spin mixing. As it was discussed in Ref. 26, the spin polarization in regions where two bands are close to each other can be approximately written as $P=\Delta/\sqrt{\Delta^2+4V_{SO}^2}$. This expression is based on the consideration of a two-level system with the spin-orbit interaction as a perturbation, where Δ is a band separation and V_{SO} is some effective spin-orbit interaction. It is evident that for **k** points with small energetic separation of a few bands, small spin polarizations are obtained. Especially, if certain **k** points have degeneracy ($\Delta=0$) in the nonrelativistic case, the spin polarization vanishes for them.

For example, a degeneracy is lifted close to the Fermi energy at the X point of Pt (Fig. 2). This leads to the spin polarization P close to zero at the Fermi surface (Fig. 4, ninth band). The same holds for the L point of the 11th band (compare Figs. 2 and 4). In the literature other examples such as Al (Ref. 26) and Co (Ref. 27) are discussed with special emphasis on the influence on experimental results. Especially, spin-flip scattering rates can be strongly influenced by this effect.

The dominant bands for Fe in a relativistic calculation are shown in Fig. 5, where the spin polarization is given as color code. The calculated Fermi surface is in very good agreement to results of Wang *et al.*[24] We obtain the same bands (5–10) but only four bands (7–10) are shown here. Since only very small pockets are formed by the bands 5 and 6, they are skipped for further discussion. From the picture of spin polarization, one can see that the nineth band is dominated by electrons with $\langle\hat{\beta}\sigma_z\rangle\simeq 1$ and the tenth band by $\langle\hat{\beta}\sigma_z\rangle\simeq -1$ only. This is obvious from a comparison to the Fermi surface of a nonrelativistic calculation shown in Fig. 6. The sixth band of the majority electrons is definitely related to the nineth band of the relativistic calculation. The same holds for the fourth minority band in Fig. 6 and the tenth band in Fig. 5. Since Fe is still a relatively light element, the relativistic treatment gives absolute values of the spin polarization close to the one (namely, $P=1$) obtained by the nonrelativistic approach with well-defined spin-up and spin-down states. For the bands 7 and 8 the result is different since they are mixtures of the fifth majority and the third minority band. In a nonrelativistic calculation both bands are well separated by the spin quantum number. Including relativistic effects, the spin is not any more conserved and the bands intermix. It is an important change that should influ-

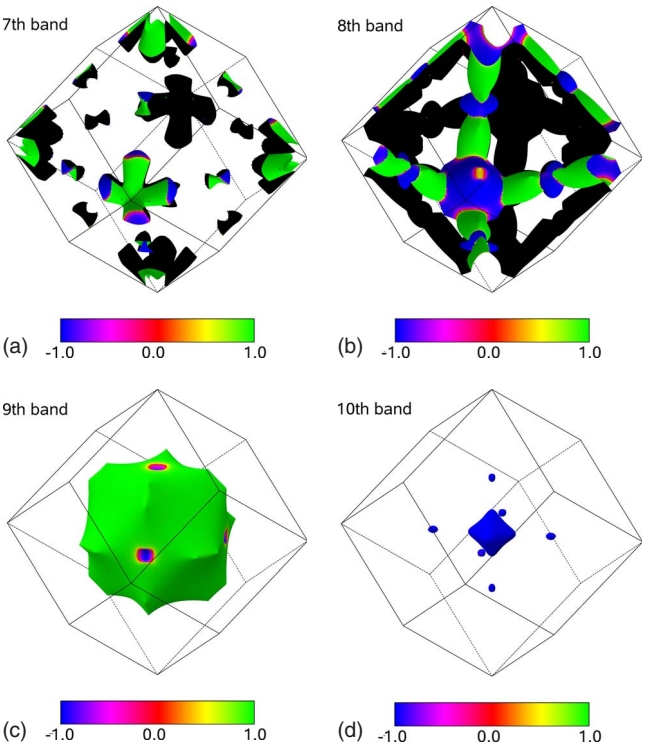

FIG. 5. (Color online) Calculated relativistic Fermi surface for the bands 7–10 of bcc Fe. The expectation values of the $\hat{\beta}\sigma_z$ operator are given as color code.

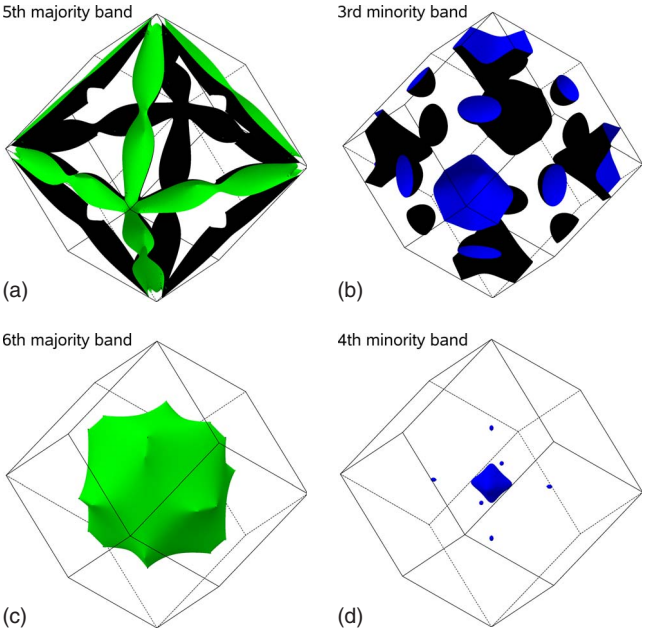

FIG. 6. (Color online) Calculated nonrelativistic Fermi surface of bcc Fe (upper left: fifth majority band, upper right: third minority, lower left: sixth majority band, and lower right: fourth minority band).

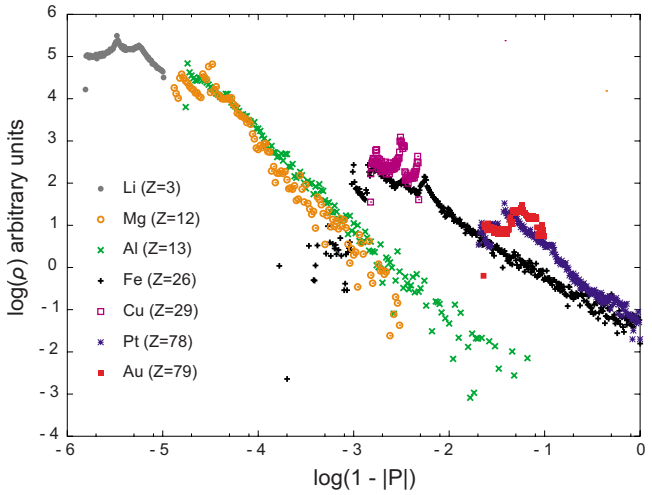

FIG. 7. (Color online) A histogram $\rho(P)$ of calculated spin mixing parameters $1-|P_k|$ on the Fermi surface of different metals on a double-logarithmic scale. Fabian and Das Sarma (Ref. 26) found for Al the same dependency by treating the spin-orbit coupling as perturbation. Lattice constants are taken from experiment: Li(bcc, a =3.509 Å), Mg(hex, a=3.210 Å), Al(fcc, a=4.050 Å), Fe(bcc, a =2.867 Å), Cu(fcc, a=3.614 Å), Pt(fcc, a=3.924 Å), and Au(fcc, a=4.078 Å). For Mg it was necessary to take a relaxed c/a ratio of 1.48 since in this system c/a is crucial to obtain the spin hot spots.

ence spin sensitive measurements. Values close to zero are obtained in small regions where the spin polarization changes sign. These states are complete mixtures of spin-up and spin-down states. For special symmetry lines this effect was discussed by Ackermann *et al.*[49] They have found the transition from spin-expectation value $\langle\hat{\beta}\sigma_z\rangle \simeq 1$ to $\langle\hat{\beta}\sigma_z\rangle \simeq -1$ at anticrossing points in Γ-H direction of Fe. However, their discussion was not focused on the **k** points at the Fermi level which are the important states for the spin-dependent electronic transport.

To compare the effect of the spin-orbit coupling in different materials, a histogram of the k-dependent spin-mixing parameter $(1-|P_k|)$ is shown in Fig. 7 [$\rho(P)$ is the probability to find states at the Fermi level with the polarization P] for Li, Mg, Al, Fe, Cu, Pt, and Au. Here we introduce k as a combined index for the band number n and the crystal momentum **k**. Li, Cu, and Au are examples with only one band at the Fermi level far from points of degeneracy. The distributions of $\rho(P)$ are very narrow for these three materials and mainly shifted by the difference in the atomic number. In contrast, the distributions for Mg, Al, Fe, and Pt are very broad with a linear slope in the double-logarithmic plot. In the case of the light elements Mg and Al, spin-mixing parameters comparable to Cu are possible. It has two reasons as explained by Fabian and Das Sarma.[26] First, Fermi-surface sheets are close to the Brillouin-zone boundaries that increases the spin mixing. Second, it is due to the crossing of bands (accidental degeneracy) at the Fermi level which leads to an increase in the spin-orbit coupling strength. As shown in Ref. 26 spin-mixing parameters up to unity can be resolved, if a very fine **k** mesh is used around the hot spots where the degeneracy is lifted. However, these points are statistically irrelevant and do not contribute significantly to

TABLE I. Averaged spin mixing parameter $\langle 1-|P_k|\rangle_k$ for different metals (scaled by a factor of 10^3).

Li	Mg	Al	Fe	Cu	Pt	Au
0.005	0.049	0.083	49	3	118	60

Fermi-surface averages. The slope of the probability amplitude $\rho(P)$ with the long tail is similar for Al and Mg and can explain a special behavior of Al and Mg in conduction electron-spin-resonance experiments.[26] For the understanding it is instructive to compare also Cu with Fe and Au with Pt. In both cases the atomic number Z is very similar for the two compared materials. Due to the multisheeted Fermi surface of Fe and Pt with several lifted degeneracies, the spin mixing parameter is strongly enhanced and the distribution is broadened. This result shows that for Fe similar effects as discussed for Co by Pickel *et al.*[27] should be measurable. They found that the spin hot spots increase the spin-relaxation process drastically.

Figure 7 reflects perfectly the situation with the assumption of well-defined spin-up and spin-down states. For light elements with a simple Fermi surface such as Li, the assumption works fine. That is quite reasonable even for Cu. In contrast, it is already questionable to assume well-defined spin states in the case of heavy materials such as Pt or polyvalent light materials such as Al. The averaged spin-mixing parameters are summarized in Table I. For Fe and Cu, the elements with comparable atomic numbers, the averaged spin mixing parameters differ by a factor of 10. It is caused by the avoided crossings of bands in Fe. For Pt and Au a similar behavior is obvious. The present results for the averaged spin mixing parameters of Fe, Cu, and Au are in good agreement with similar calculations published recently.[28]

IV. CONCLUSION

We present the implementation of relativistic band structure, Fermi surface, and wave-function calculations in the relativistic screened KKR method. By means of these quantities, the spin polarization on the Fermi surface of several metals is discussed. Such information is important for a theoretical analysis of spin and electronic transports. It is shown that for monovalent metals such as Li, Cu, and Au, the "up" and "down" spin-polarized states are well defined for all **k** points on the Fermi surface. Whereas for polyvalent materials such as Mg, Al, Fe, and Pt, electron states with zero spin polarization exist. The effect is drastic in the case of heavy elements where large regions with vanishing spin polarization exist. As an additional mechanism, spin hot spots occur for magnetic materials such as Fe at the avoided crossing points of the exchange-split bands. For such materials it can be essential to take relativistic effects into account for a proper description of spin-dependent phenomena. In addition, an appropriate method to treat the spin polarization of degenerate bands in nonmagnetic materials is proposed.

ACKNOWLEDGMENTS

This work was partially supported by the Deutsche

Forschungsgemeinschaft (SFB 762). M. Gradhand is a member of the International Max Planck Research School for Science and Technology of Nanostructures.

APPENDIX: TRANSFORMATION TO A GLOBAL QUANTIZATION AXIS

In order to apply the transformation given by Eqs. (9) and (10), we need to calculate matrix elements such as

$$\begin{aligned}\langle\Psi_{n\mathbf{k}}|\hat{\beta}\sigma_z|\Psi_{n'\mathbf{k}}\rangle &= -\sum_{\kappa'\mu'}\sum_{\kappa''\mu''} a^{n*}_{\kappa'\mu'}(\mathbf{k})a^{n'}_{\kappa''\mu''}(\mathbf{k}) \\ &\times\sum_{\kappa\mu}\Bigg\{\left(\frac{2\mu}{2\kappa+1}\right)\int g^{*}_{\kappa\mu;\kappa'\mu'}(r)g_{\kappa\mu;\kappa''\mu''}(r)r^2dr \\ &+\frac{2\mu}{2\kappa-1}\int f^{*}_{\kappa\mu;\kappa'\mu'}(r)f_{\kappa\mu;\kappa''\mu''}(r)r^2dr \\ &+\sqrt{1-\left(\frac{2\mu}{2\kappa+1}\right)^2}\int g^{*}_{\kappa\mu;\kappa'\mu'}(r)g_{-\kappa-1,\mu;\kappa''\mu''}(r)r^2dr \\ &-\sqrt{1-\left(\frac{2\mu}{2\kappa-1}\right)^2}\int f^{*}_{\kappa\mu;\kappa'\mu'}(r)f_{-\kappa+1,\mu;\kappa''\mu''}(r)r^2dr\Bigg\},\end{aligned} \tag{A1}$$

$$\begin{aligned}\langle\Psi_{n\mathbf{k}}|\hat{\beta}\sigma_+|\Psi_{n'\mathbf{k}}\rangle &= -\sum_{\kappa'\mu'}\sum_{\kappa''\mu''} a^{n*}_{\kappa'\mu'}(\mathbf{k})a^{n'}_{\kappa''\mu''}(\mathbf{k})\sum_{\kappa\mu}\Bigg\{\sqrt{\kappa^2-1/4-\mu(\mu-1)} \\ &\times\left[\frac{2}{2\kappa+1}\int g^{*}_{\kappa\mu;\kappa'\mu'}(r)g_{\kappa\mu-1;\kappa''\mu''}(r)r^2dr\right. \\ &\left.+\frac{2}{2\kappa-1}\int f^{*}_{\kappa\mu;\kappa'\mu'}(r)f_{\kappa\mu-1;\kappa''\mu''}(r)r^2dr\right] \\ &+\frac{\sqrt{(2\kappa+1-2\mu)(2\kappa+3-2\mu)}}{2\kappa+1} \\ &\times\int g^{*}_{\kappa\mu;\kappa'\mu'}(r)g_{-\kappa-1,\mu-1;\kappa''\mu''}(r)r^2dr \\ &+\frac{\sqrt{(2\kappa-1+2\mu)(2\kappa-3+2\mu)}}{2\kappa-1} \\ &\times\int f^{*}_{\kappa\mu;\kappa'\mu'}(r)f_{-\kappa+1,\mu-1;\kappa''\mu''}(r)r^2dr\Bigg\},\end{aligned} \tag{A2}$$

and

$$\begin{aligned}\langle\Psi_{n\mathbf{k}}|\hat{\beta}\sigma_-|\Psi_{n'\mathbf{k}}\rangle &= -\sum_{\kappa'\mu'}\sum_{\kappa''\mu''} a^{n*}_{\kappa'\mu'}(\mathbf{k})a^{n'}_{\kappa''\mu''}(\mathbf{k})\sum_{\kappa\mu} \\ &\times\Bigg\{\sqrt{\kappa^2-1/4-\mu(\mu+1)} \\ &\times\left[\frac{2}{2\kappa+1}\int g^{*}_{\kappa\mu;\kappa'\mu'}(r)g_{\kappa\mu+1;\kappa''\mu''}(r)r^2dr\right. \\ &\left.+\frac{2}{2\kappa-1}\int f^{*}_{\kappa\mu;\kappa'\mu'}(r)f_{\kappa\mu+1;\kappa''\mu''}(r)r^2dr\right] \\ &-\frac{\sqrt{(2\kappa+1+2\mu)(2\kappa+3+2\mu)}}{2\kappa+1} \\ &\times\int g^{*}_{\kappa\mu;\kappa'\mu'}(r)g_{-\kappa-1,\mu+1;\kappa''\mu''}(r)r^2dr \\ &-\frac{\sqrt{(2\kappa-1-2\mu)(2\kappa-3-2\mu)}}{2\kappa-1} \\ &\times\int f^{*}_{\kappa\mu;\kappa'\mu'}(r)f_{-\kappa+1,\mu+1;\kappa''\mu''}(r)r^2dr\Bigg\}.\end{aligned} \tag{A3}$$

The expressions above are written in a general form valid for nonmagnetic as well as magnetic systems. Actually, in the nonmagnetic case, they can be simplified due to the dependence of the radial solutions on κ only.[38] Thus, with $n'=n$ in Eq. ((A1), we have the expression for the spin polarization used in our calculations.

The implementation of the ladder operators $\sigma_+=\sigma_x+i\sigma_y$ and $\sigma_-=\sigma_x-i\sigma_y$ in Eqs. ((A2) and (A3) provides us an easier way for dealing with the conditions given by Eq. (10). Finally, we can write the coefficients of the transformation in Eqs. (9) and (10) in the following form:

$$c_1=\frac{1}{\sqrt{2}}\sqrt{1+\frac{|a|}{\sqrt{|a|^2+4|d|^2}}} \tag{A4}$$

and

$$c_2=-\left(\frac{|a|}{a}\right)\frac{d\sqrt{2}}{\sqrt{|a|^2+4|d|^2+|a|\sqrt{|a|^2+4|d|^2}}}, \tag{A5}$$

where the parameters a and d are given by

$$a=2i\ \mathrm{Im}\{\langle\Psi^1_k|\hat{\beta}\sigma_y|\Psi^2_k\rangle\langle\Psi^2_k|\hat{\beta}\sigma_x|\Psi^1_k\rangle\} \tag{A6}$$

and

$$d=\langle\Psi^2_k|\hat{\beta}\sigma_x|\Psi^1_k\rangle\langle\Psi^1_k|\hat{\beta}\sigma_y|\Psi^1_k\rangle-\langle\Psi^2_k|\hat{\beta}\sigma_y|\Psi^1_k\rangle\langle\Psi^1_k|\hat{\beta}\sigma_x|\Psi^1_k\rangle. \tag{A7}$$

Here we use $c_1=|c_1|$ as the choice of an arbitrary phase, which does not influence the results.

*martin.gradhand@physik.uni-halle.de

[1] F. J. Jedema, A. T. Filip, and B. J. van Wees, Nature (London) **410**, 345 (2001).
[2] H. Kurt, R. Loloee, K. Eid, W. P. Pratt, J. Bass, and J. Bass, Appl. Phys. Lett. **81**, 4787 (2002).
[3] S. O. Valenzuela and M. Tinkham, Nature **442**, 176 (2006).
[4] L. Vila, T. Kimura, and Y. C. Otani, Phys. Rev. Lett. **99**, 226604 (2007).
[5] T. Seki, Y. Hasegawa, S. Mitani, S. Takahashi, H. Imamura, S. Maekawa, J. Nitta, and K. Takanashi, Nature Mater. **7**, 125 (2008).
[6] T. Yang, T. Kimura, and Y. Otani, Nat. Phys. **4**, 851 (2008).
[7] M. N. Baibich, J. M. Broto, A. Fert, F. Nguyen Van Dau, F. Petroff, P. Etienne, G. Creuzet, A. Friederich, and J. Chazelas, Phys. Rev. Lett. **61**, 2472 (1988).
[8] G. Binasch, P. Grünberg, F. Saurenbach, and W. Zinn, Phys. Rev. B **39**, 4828 (1989).
[9] M. Julliere, Phys. Lett. A **54**, 225 (1975).
[10] J. S. Moodera, L. R. Kinder, T. M. Wong, and R. Meservey, Phys. Rev. Lett. **74**, 3273 (1995).
[11] T. S. Plaskett, P. P. Freitas, N. P. Barradas, M. F. da Silva, and J. C. Soares, J. Appl. Phys. **76**, 6104 (1994).
[12] S. Yuasa, T. Nagahama, A. Fukushima, Y. Suzuki, and K. Ando, Nature Mater. **3**, 868 (2004).
[13] J. Slonczewski, J. Magn. Magn. Mater. **159**, L1 (1996).
[14] M. Tsoi, A. G. M. Jansen, J. Bass, W.-C. Chiang, M. Seck, V. Tsoi, and P. Wyder, Phys. Rev. Lett. **80**, 4281 (1998).
[15] E. B. Myers, D. C. Ralph, J. A. Katine, R. N. Louie, and R. A. Buhrman, Science **285**, 867 (1999).
[16] J. A. Katine, F. J. Albert, R. A. Buhrman, E. B. Myers, and D. C. Ralph, Phys. Rev. Lett. **84**, 3149 (2000).
[17] M. I. Dyakonov and V. I. Perel, JETP Lett. **35A**, 459 (1971).
[18] Y. K. Kato, R. C. Myers, A. C. Gossard, and D. D. Awschalom, Science **306**, 1910 (2004).
[19] A. Crépieux and P. Bruno, Phys. Rev. B **64**, 014416 (2001).
[20] T. Tanaka, H. Kontani, M. Naito, T. Naito, D. S. Hirashima, K. Yamada, and J. Inoue, Phys. Rev. B **77**, 165117 (2008).
[21] Y. Tian, L. Ye, and X. Jin, Phys. Rev. Lett. **103**, 087206 (2009).
[22] T. Miyasato, N. Abe, T. Fujii, A. Asamitsu, S. Onoda, Y. Onose, N. Nagaosa, and Y. Tokura, Phys. Rev. Lett. **99**, 086602 (2007).
[23] F. D. M. Haldane, Phys. Rev. Lett. **93**, 206602 (2004).
[24] X. Wang, D. Vanderbilt, J. R. Yates, and I. Souza, Phys. Rev. B **76**, 195109 (2007).
[25] N. Tombros, S. Tanabe, A. Veligura, C. Jozsa, M. Popinciuc, H. T. Jonkman, and B. J. van Wees, Phys. Rev. Lett. **101**, 046601 (2008).
[26] J. Fabian and S. Das Sarma, Phys. Rev. Lett. **81**, 5624 (1998).
[27] M. Pickel, A. B. Schmidt, F. Giesen, J. Braun, J. Minár, H. Ebert, M. Donath, and M. Weinelt, Phys. Rev. Lett. **101**, 066402 (2008).
[28] D. Steiauf and M. Fähnle, Phys. Rev. B **79**, 140401(R) (2009).
[29] S. Takada, Prog. Theor. Phys. **36**, 224 (1966).
[30] Y. Onodera and M. Okazaki, J. Phys. Soc. Jpn. **21**, 1273 (1966).
[31] R. Feder, F. Rosicky, and B. Ackermann, Z. Phys. B **52**, 31 (1983).
[32] P. Strange, R. Staunton, and B. L. Gyorffy, J. Phys. C **17**, 3355 (1984).
[33] G. Schadler, P. Weinberger, A. M. Boring, and R. C. Albers, Phys. Rev. B **34**, 713 (1986).
[34] S. A. Ostanin and V. P. Shirokovskii, J. Phys.: Condens. Matter **2**, 7585 (1990).
[35] L. Szunyogh, B. Újfalussy, and P. Weinberger, Phys. Rev. B **51**, 9552 (1995).
[36] P. Strange, *Relativistic Quantum Mechanics* (Cambridge University Press, Cambridge, England, 1998).
[37] H. Ebert, *Electronic Structure and Physical Properties of Solids, Lecture Notes in Physics* (Springer, Berlin, 2000), Vol. 535, p. 191.
[38] J. Zabloudil, R. Hammerling, L. Szunyogh, and P. Weinberger, *Electron Scattering in Solid Matter* (Springer-Verlag, Berlin, 2005).
[39] R. Zeller, P. H. Dederichs, B. Ujfalussy, L. Szunyogh, and P. Weinberger, Phys. Rev. B **52**, 8807 (1995).
[40] N. Papanikolaou, R. Zeller, and P. H. Dederichs, J. Phys.: Condens. Matter **14**, 2799 (2002).
[41] S. H. Vosko, L. Wilk, and M. Nusair, Can. J. Phys. **58**, 1200 (1980).
[42] H. Ebert, H. Freyer, A. Vernes, and G. Y. Guo, Phys. Rev. B **53**, 7721 (1996).
[43] P. Zahn, Ph.D. thesis, Technische Universität Dresden, 1998.
[44] R. J. Elliott, Phys. Rev. **96**, 266 (1954).
[45] H. A. Kramers, Proc. R. Acad. Sci. Amsterdam **33**, 959 (1930).
[46] S. Bei der Kellen and A. J. Freeman, Phys. Rev. B **54**, 11187 (1996).
[47] P. Strange, H. Ebert, J. B. Staunton, and B. L. Gyorffy, J. Phys.: Condens. Matter **1**, 2959 (1989).
[48] X. Wang, J. R. Yates, I. Souza, and D. Vanderbilt, Phys. Rev. B **74**, 195118 (2006).
[49] B. Ackermann, R. Feder, and E. Tamura, J. Phys. F: Met. Phys. **14**, L173 (1984).